geoconvention
Virtual Event 2020
September 21-23
CSPG • CSEG • CWLS • GAC • MAC • IAH

Seismic Trace Interpolation using Residual Dense Network

Hongliang Zhang, Amr Ibrahim, Daniel Trad and Kristopher Innanen
CREWES Project, Department of Geoscience, University of Calgary

Summary

A CNN-based residual dense network (RDNet) is utilized to interpolate missing seismic traces within 2D synthetic seismic data. The contiguous memory mechanism, residual learning and feature fusion in both local and global levels enable RDNet to interpolate regularly missing traces with relatively high recovered S/N and accommodate spatial aliasing. In cases of randomly missing traces, RDNet produces comparable though slightly degraded results relative to the conventional minimum weighted norm inversion. Reliable results are obtained with less missing data, e.g., recovered signal-to-noise ratio (S/N) of ~ 40 dB and 30 dB for 10% and 30% randomly missing traces, respectively. As the missing-trace percentage increases, errors accrue in regions of the data with big gaps (typically larger than five consecutive traces). We expect this will be improved by including more training data, which is currently being examined.

Introduction

Investigations of interpolation methods have been documented in a number of previous studies, which mainly differ in complexity, assumptions, operator size, and the mathematical/numerical engine used (Trad, 2009). Generally, these interpolation techniques can be classified into four categories: prediction filter-based approach (Spitz, 1991; Naghizadeh and Sacchi, 2007), wave-equation based approach (Ronen, 1987), mathematical transform-based approach (Chen et al., 2014; Gan et al., 2015; Ibrahim et al., 2018) and rank-reduction-based approach (Oropeza and Sacchi, 2011; Ma, 2013; Kreimer et al., 2013).

Recently, as a subset of artificial intelligence, machine learning (ML) has grown rapidly in popularity and effectiveness, as the result of improvements in the computational capacity of computers and rapid developments within the big data revolution. At present a big push is underway to formulate and examine algorithms for processing, inversion, and interpretation of seismic data which take advantage of the optimizations and "learning" capacities of AI and ML. Not only are we motivated by the possibility of extending the accuracy and reach of existing algorithms by doing so, but also by the fact that properly-formulated ML processing fits straightforwardly and naturally into new and future computing architectures and hardware technology. Thus, even a reproduction of an existing seismic processing approach within the context of ML represents an important step. Researchers have attempted to formulate interpolation within the ML environment in recent years.

In this work, we will apply the residual dense network (RDNet), a convolutional neural network normally used for the image super-resolution problem, to the interpolation of missing seismic traces. Using the synthetic seismic data and RDNet, we will then investigate the application to the cases with regularly and randomly missing traces and compare with results obtained using an existing conventional interpolation algorithm and the other convolutional neural network (CNN)-based approach (i.e. minimum weighted norm inversion (MWNI) and ResNet).

Method

The residual dense network (RDNet) was originally designed for image super-resolution (Zhang et al., 2018), which can make full use of hierarchical features from original low-resolution images. Here, we take the seismic interpolation as an image super-resolution problem and will adopt a similar RDNet as the study of Zhang et al. (2018) for seismic interpolation. Figure 1 shows the architecture of the RDNet, in which the input is seismic data with missing traces, and output is the data after interpolation. The outputs of a preceding block and each layer within the current block connect to all the subsequent layers directly through the so-called contiguous memory mechanism. In addition, there is a concatenation operation at the end of each residual dense block, which is designed for adaptively fusing the states of preceding blocks and all the layers in the current block. Furthermore, the local residual learning is also included in each block for further improving the representation ability of the neural network. As shown in Figure 1, the feature fusion and residual learning are also designed in a global way, and this feature fusion can extract global features by fusing the states from all the residual dense blocks. For the sake of comparison, interpolations are also implemented with a previously proposed residual network (ResNet) (Wang et al., 2019) and a minimum weighted norm inversion (MWNI) (Liu and Sacchi, 2004).

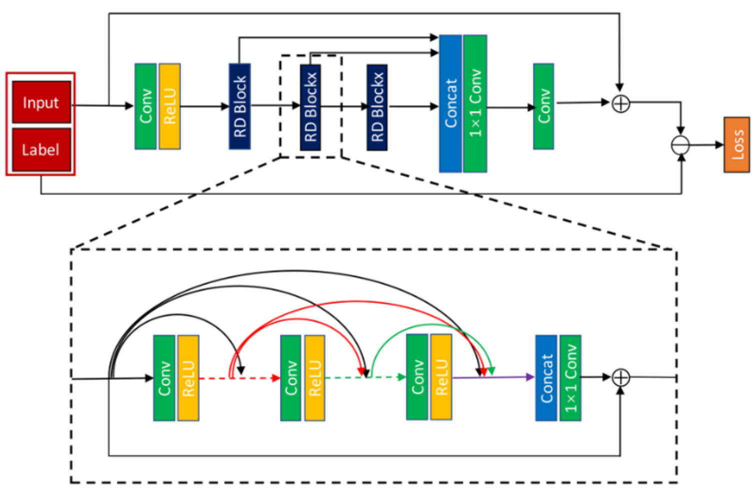

Figure 1 The architecture of the RDNet used in this study (modified from Zhang et al., 2018).

Dataset and RDNet Training

To test the effectiveness of RDNet on seismic interpolation, we use 2D synthetic seismic data generated by finite differences from the velocity model in Figure 2, which contains flat, dipping, curved layer interfaces, and two salt bodies with higher velocities compared with surrounding medium. Altogether, 146 shot gathers are generated, and each has 513 surface receivers. In the network training, 80% of shot records are used for training and 20% for validation. To further test the flexibility of the trained RDNet on other datasets, we also generated shot gathers from other two velocity models, one of which is a layered velocity model, and the other has two thin embedded layers.

The RDNet is trained with Keras using the synthetic dataset. The loss function is defined as the mean squared error (MSE) between the interpolated and labeled data. In the neural network training, the evaluation metric is defined as the recovered signal to noise ratio (S/N) in dB, and the Adaptive momentum algorithm (Adam) (Kingma and Ba, 2014) is used to update and search the optimal parameters. In the training stage, the maximum training step number is set to be 150, and the initial learning rate is set as 1E-4 after testing a series of values. The learning rate decreases with training step, and its value is reduced by 5% after each epoch. We also adopt an early stopping scheme in the training stage, i.e., the training will stop if there is no improvement in the S/N of validation set after 10 consecutive epochs. Similar to the procedure adopted in the ResNet training (Wang et al., 2019), we break each seismic shot gather into small patches for training with 50% overlap between two adjacent patches in both spatial and temporal directions. Due to the limited GPU memory, we use the mini-batch to update parameters in each iteration.

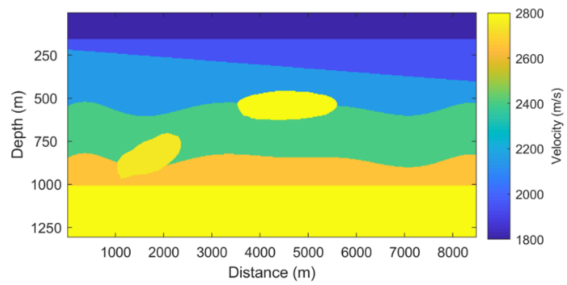

Figure 2 Velocity model used to generate the training and validation data.

Results

Table 1 Average recovered S/N (in dB) using three interpolation methods based on the synthetic data.

Interpolation Methods		Regularly Missing Cases		Randomly Missing Cases		
		1/2 of the original trace spacing	1/3 of the original trace spacing	10% missing traces	30% missing traces	50% missing traces
MWNI	Train Set	33.7	15.0	47.2	33.9	25.0
	Validation Set	33.8	14.6	47.3	33.7	25.2
	Test Set	32.0	13.2	42.7	34.4	21.7
ResNet	Train Set	36.5	27.9	N/A	N/A	N/A
	Validation Set	36.5	28.1	N/A	N/A	N/A
	Test Set	35.1	25.8	N/A	N/A	N/A
RDNet	Train Set	45.4	37.3	41.5	31.9	22.5
	Validation Set	45.2	37.2	40.9	30.2	21.7
	Test Set	42.5	31.4	41.1	31.7	22.7

Interpolation results for both regularly and randomly missing cases are summarized in Table 1. It can be noticed that RDNet outperforms the other two approaches in the case of regularly missing cases, and the reconstruction errors from MWNI are the largest among the three especially for the case with spatial aliasing. A series of synthetic experiments demonstrates that both RDNet and ResNet can handle the aliasing problem effectively (Figure 3). In the cases of randomly missing traces, we observe that the recovered S/Ns using RDNet are close to or slightly lower than those obtained using MWNI. In addition, with the missing percentage exceeding 30%, reconstruction errors for some certain shots mainly exhibit in areas where there are relatively large trace gaps (typically > 5 consecutive traces) (Figure 4). Theoretically, the number of combinations for selecting 30% or 50% out of 512 traces is much larger than that for selecting 10%, however, training data sizes for these three cases are the same, which may result in the insufficient training samples for these scenarios.

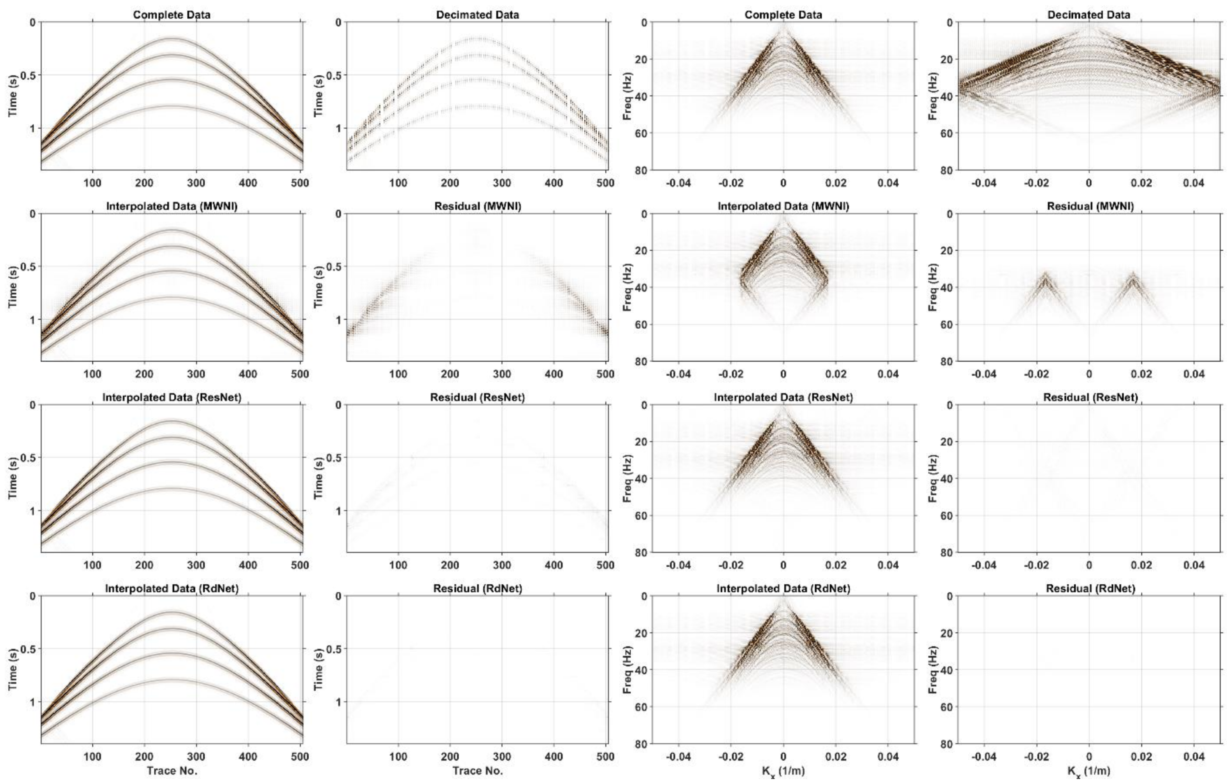

Figure 3 Interpolation results for test shot # 1 for the case of interpolating two traces between every two adjacent traces. S/Ns for the reconstructed shot gather using the three methods are 10.9, 27.7 and 35.2 dB, respectively.

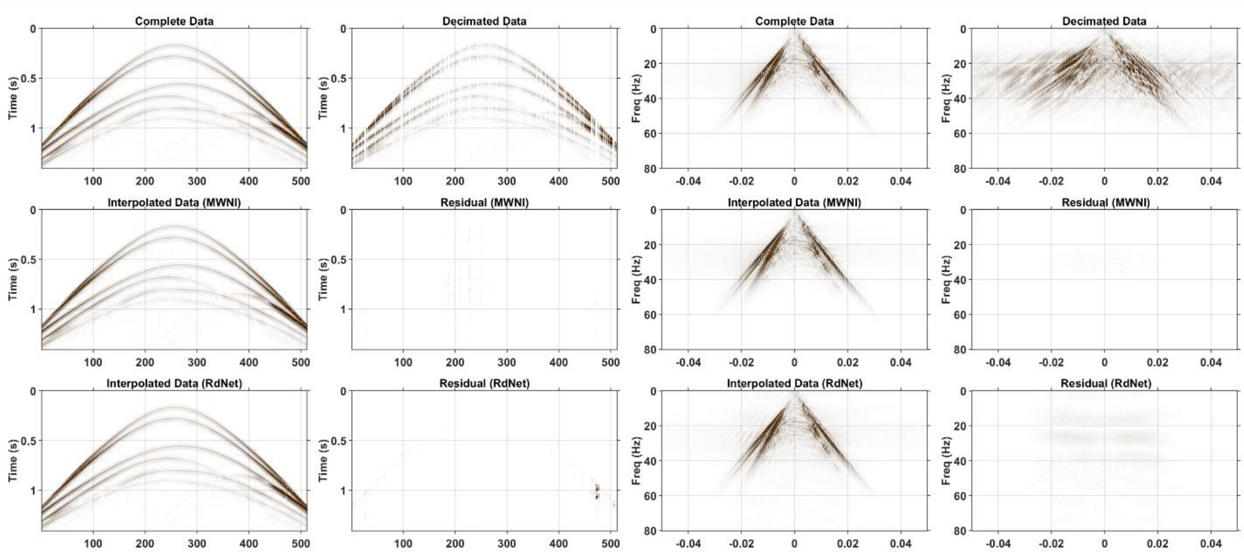

Figure 4 Interpolation results for validation shot # 2 using MWNI (2nd row) and RDNet (3rd row) for the case of 30% missing traces. S/Ns for the reconstructed shot gather using these two methods are 32.7 and 18.1 dB, respectively.

Conclusions

A series of synthetic experiments indicate that RDNet could reconstruct the missing seismic traces with relatively higher recovered S/N for regularly missing cases compared with MWNI and ResNet. Its effectiveness in handling the spatial aliasing effects has also been demonstrated. In terms of the randomly missing cases, RDNet could achieve interpolation results with recovered S/N close to or slightly lower than conventional MWNI. When the training dataset is insufficient (missing traces exceed 30%), reconstruction errors using RDNet for some certain shots mainly exhibit in areas with large trace gaps (typically > 5 consecutive traces). This issue is expected to be solved in future work by including more data during the training phase.

Acknowledgements

This work was funded by CREWES industrial sponsors and NSERC (Natural Science and Engineering Research Council of Canada) through the grant CRDPJ 461179-13. This research was also undertaken thanks in part to funding from the Canada First Research Excellence Fund.

References

Chen, Y., Chen, K., Shi, P., andWang, Y., 2014, Irregular seismic data reconstruction using a percentile-half-thresholding algorithm: Journal of Geophysics and Engineering, **11**(6), 065001.

Gan, S., Wang, S., Chen, Y., Zhang, Y., and Jin, Z., 2015, Dealiased seismic data interpolation using seislet transform with low-frequency constraint: IEEE Geoscience and Remote Sensing Letters, **12**(10), 2150-2154.

Ibrahim, A., Terenghi, P. and Sacchi, M. D., 2018, Simultaneous reconstruction of seismic reflection and diffractions using a global hyperbolic Radon disctionary: Geophysics, **83**(6), V315-V323.

Kingma, D. P., and Ba, J., 2014, Adam: A method for stochastic optimization: arXiv preprint arXiv:1412.6980.

Kreimer, N., Stanton, A., and Sacchi, M. D., 2013, Tensor completion based on nuclear norm minimization for 5D seismic data reconstruction: Geophysics, **78**(6), V273-V284.

Liu, B., and Sacchi, M. D., 2004, Minimum weighted norm interpolation of seismic records: Geophysics, **69**(6), 1560-1568.

Ma, J., 2013, Three-dimensional irregular seismic data reconstruction via low-rank matrix completion: Geophysics,**78**(5), V181-V192.

Naghizadeh, M., and Sacchi, M. D., 2007, Multistep autoregressive reconstruction of seismic records: Geophysics, **72**(6), V111–V118.

Oropeza, V., and Sacchi, M., 2011, Simultaneous seismic data denoising and reconstruction via multichannel singular spectrum analysis: Geophysics, **76**(3), V25-V32.

Ronen, J., 1987, Wave-equation trace interpolation: Geophysics, **52**(7), 973-984.

Spitz, S., 1991, Seismic trace interpolation in the f-x domain: Geophysics, **56**(6), 785-794.

Trad, D., 2009, Five-dimensional interpolation: Removing from acquisition constraints: Geophysics, **74**(6), V123-V132.

Wang, B., Zhang, N., Lu, W., and Wang, J., 2019, Deep-learning-based seismic data interpolation: A preliminary result: Geophysics, **84**(1), V11-V20.

Zhang, Y., Tian, Y., Kong, Y., Zhong, B., and Fu, Y., 2018, Residual dense network for image super-resolution, *in* Proceedings of the IEEE Conference on Computer Vision and Pattern Recognition, 2472-2481.